

Quantifying the Level of Intermacromolecular Interactions in Ethylene-Propylene Copolymers by Using Pyrene Excimer Formation

Solmaz Pirouz, Jean Duhamel*

Waterloo Institute for Nanotechnology, Institute for Polymer Research, Department of Chemistry, University of Waterloo, Waterloo, ON N2L 3G1, Canada

Sheng Jiang, Akhilesh Duggal[§]

Afton Chemical Corporation, 500 Spring Street, Richmond, VA 23219, USA

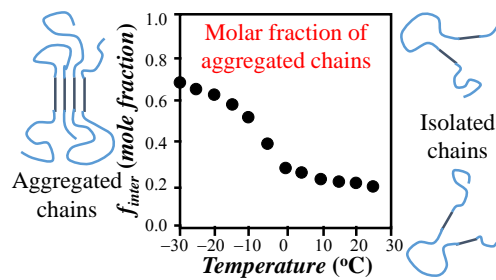
* To whom correspondence should be addressed.

§ Current address: ExxonMobil Corporation, 600 Billingsport Road, Paulsboro, NJ 08066

ABSTRACT

A unique methodology based on fluorescence measurements is introduced to quantitatively measure the actual level of interpolymeric association between ethylene-propylene (EP) copolymers used as viscosity index improvers (VIIs) in engine oils. To this end, two EP copolymers, one amorphous (EP(AM)) and the other semicrystalline (EP(SM)), were maleated and then fluorescently labeled with 1-pyrenemethylamine and 2-(2-naphthyl)ethylamine to yield Py-EP and Np-EP, respectively. Successful maleation and fluorescence labeling were confirmed by Fourier transform infrared (FTIR) spectroscopy. Level of crystallinity of the EP copolymers were inferred from FTIR, carbon nuclear magnetic resonance (^{13}C NMR), and differential scanning calorimetry (DSC) experiments. The solution behaviour of the EP copolymers was characterized by conducting intrinsic viscosity measurements as a function of temperature to define the temperature range where fluorescence studies should be conducted. Fluorescence resonance energy transfer (FRET) experiments were used to demonstrate the existence of interpolymeric associations, but a quantitative measure of the actual level of association, such as the molar fraction of interpolymeric interaction (f_{inter}) between EP copolymers, could not be determined by FRET. However, taking advantage of the fact that the fluorescence intensity ratio I_E/I_M of excimer-to-monomer is directly proportional to the local pyrene concentration $[Py]_{\text{loc}}$ of a pyrene-labeled polymer, a quantitative measure of the actual level of intermolecular association was obtained by measuring the I_E/I_M ratio. Results showed that f_{inter} of pyrene-labeled EP(SM) increased upon decreasing the temperature and increasing the polymer concentration as would have been expected from such a polymer. This result suggests that pyrene excimer formation provides a reliable method to quantitatively determine f_{inter} for EP copolymers used as VIIs, an information which is otherwise difficult to extract from standard FRET experiments.

For Table of Contents use only



Quantifying the Level of Intermacromolecular Interactions in Ethylene-Propylene Copolymers by Using Pyrene Excimer Formation

Solmaz Pirouz, Jean Duhamel, Sheng Jiang, Akhilesh Duggal

INTRODUCTION

Engine oils provide the necessary lubrication between the moving parts of engines, and as a result, are vital to all internal combustion powered vehicles. Viscosity index improvers (VIIs), dispersants, detergents, antioxidants, and antiwear components are chemicals that are deliberately added to engine oils to enhance oil performance during the operation of engines.¹ In particular, VIIs are added to the oil to reduce the inherent decrease in oil viscosity that occurs with increasing temperature. Without VIIs, the oil would be too thin at high temperature to properly coat the engine parts, thus undermining its lubricating purpose, and too viscous to flow at low temperature, resulting in a lack of lubrication and possible seizure of the engine parts. VIIs are designed to counteract the reduction in oil viscosity observed at high engine temperatures without excessively increasing the viscosity of the oil at lower temperatures.²⁻⁴ Thus, VIIs play a key role in substantially enhancing the oil efficiency and durability while providing maximum engine protection.^{5,6}

Synthetic polymers, such as polymethacrylates, ethylene-propylene copolymers (EP), and hydrogenated styrene-diene copolymers have been used as VIIs by taking advantage of the unique polymer coil expansion undergone by these polymers with increasing solution temperature.^{4,7-9} Among these polymers, EP copolymers were first introduced as a lubricant additive by Exxon in the late 1960s.¹⁰ The ethylene-to-propylene ratio in EP copolymers defines the quality of such a polymer as a VII.⁷ High ethylene contents of 50-70 mol% provide optimum oil thickening and oxidative stability.¹¹ However, at low temperature, such high ethylene contents lead to polymer crystallization and thus insolubility, and strong interactions with wax, an ubiquitous component of base oils.¹¹ Despite these drawbacks, semicrystalline EP copolymers are being used as VIIs due to their ability to undergo a coil expansion with increasing

temperature. As a matter of fact, an oligoethylene sequence within a semicrystalline EP copolymer will crystallize at low temperature and form dense crystalline microdomains, resulting in polymer coils having small hydrodynamic volumes (V_h). Increasing the solution temperature melts the crystalline microdomains which results in a higher V_h for the polymer coils. Since the viscosity of the solution depends on the volume-fraction of the solution that is occupied by the polymer coils, an expansion of the polymer coil leads to a viscosity increase. Therefore, the decrease in engine oil viscosity that follows an increase in temperature is mitigated by the expansion of the polymer coils associated with the melting of the crystalline microdomains. By comparison, the change in V_h with temperature is less sudden and more progressive for amorphous EP copolymers so that the viscosity of their solution is less affected by temperature. The effect of ethylene content of an EP copolymer on the temperature dependency of V_h has been well documented.^{3,4}

So far, the variation of V_h with temperature has been discussed in terms of an intramolecular phenomenon happening with semicrystalline EP copolymers. However the formation of microcrystals in solution indicates that polymer-polymer interactions are favored over polymer-solvent interactions. In other words, the polymer becomes less soluble, a condition which normally leads to uncontrolled interpolymeric aggregation and eventually precipitation of the polymer. In the case of an engine oil, precipitation of a VII from the oil would have catastrophic consequences on the lubrication performance of the oil. These observations lead to the conclusion that the characterization of the extent of polymeric associations in solution, and the study of the chemicals known to affect them, is of paramount interest to the lubricant oil-additive industry.

Fluorescence techniques based on Fluorescence Resonance Energy Transfer (FRET), pyrene excimer formation, and to a much lesser extent fluorescence anisotropy have been instrumental in demonstrating interpolymeric interactions in solution.¹² Without exception, these techniques require that the fluorophores be tightly bound to the macromolecules of interest which in the case of solutions of EP copolymers in organic solvents necessitates that the fluorophore be covalently attached to the EP copolymer. This constraint represents a challenge for EP copolymers which are difficult to modify since their chemical stability under harsh conditions make them highly desirable polymers to work under extreme conditions such as in engine oils.¹⁰ One of the first examples of covalent attachment of pyrene onto a polyethylene (PE) film was achieved by immersing the film in a concentrated pyrene solution in chloroform overnight, removing the chloroform under a flow of nitrogen, and irradiating the pyrene-doped film under UV-light.¹³ This procedure introduced pyrene labels in the amorphous domains of the PE film and was followed by other variations. For instance, thermal decomposition of 9-anthryldiazomethane in a PE film also led to the covalent attachment of anthryl groups onto PE chains.¹⁴ PE films have also been hydroxylated by reaction with dibenzothiophene 5-oxide followed by reaction with 2-naphthoyl chloride.¹⁵ More recently, a naphthalene nitroxide, namely 4-(1-naphthoate)-2,2,6,6-tetramethylpiperidine-1-oxyl, was covalently attached onto a polyolefin in the melt in the presence of a radical initiator.¹⁶ EP copolymers have also been fluorescently labeled by maleating the EP backbone in solution with a radical initiator followed by reaction of the resulting succinic anhydride group with a fluorophore bearing an amine substituent.¹⁷ This procedure introduced by Jao et al. in 1992 takes advantage of the maleation chemistry well-known in the oil additive industry to prepare succinimide polymeric dispersants

based on polyisobutylene or EP copolymers.¹⁸ It is this last procedure that was applied in the present study to label EP copolymers with pyrene and naphthalene.

One of the tools most commonly applied to probe intermolecular associations is fluorescence resonance energy transfer (FRET), which explains its intensive use to study polymeric systems.^{2,12,19,20} Since an excited donor (D) transfers its energy to a ground-state acceptor (A) most effectively if the distance separating D from A (d_{D-A}) is less than twice the Förster radius (R_0) which is itself less than 10 nm for any given D - A pair, evidence of FRET between a D - and an A -labeled macromolecule provides strong evidence of intermacromolecular interactions. The strength of these interactions can be inferred qualitatively from the FRET efficiency (E_{FRET}) with E_{FRET} taking values between zero and unity depending on how d_{D-A} averaged over all D - A pairs compares to R_0 . Interestingly, a quantitative measure of the actual level of association, such as the molar fraction (f_{inter}) of macromolecules involved in intermolecular associations, is rarely provided when FRET is used, probably because of the complex relationship that exists between efficiency of energy transfer (E_{FRET}) and the distribution of d_{D-A} values when D and A are subject to Brownian motions in solution, as well as the unavoidable contamination of the acceptor fluorescence signal by direct excitation of the acceptor.

By comparison, we provide herein evidence that f_{inter} can be determined in a simple and straightforward manner from the fluorescence intensity ratio I_E/I_M of excimer-to-monomer obtained from the fluorescence spectrum of pyrene-labeled macromolecules. These experiments take advantage of the ability of an excited pyrene to form an excimer *on contact* upon encounter with a ground-state pyrene.²¹ Since the fluorescence intensity ratio I_E/I_M is directly proportional to the local pyrene concentration $[Py]_{\text{loc}}$, an increase in I_E/I_M reflects an increase in $[Py]_{\text{loc}}$ which

would follow from intermolecular associations.²²⁻²⁶ Comparison of the I_E/I_M ratio obtained at low and high pyrene concentration when pyrene excimer formation occurs, respectively, intra- and intermolecularly yields f_{inter} which can be used to probe the level of interpolymeric interactions. This study describes how these concepts can be applied to determine f_{inter} for two EP copolymers.

EXPERIMENTAL

Chemicals. Acetone (HPLC grade), dodecane (anhydrous, 99%), toluene (HPLC, 99.9%), biphenyl (99%), maleic anhydride (98%), succinic anhydride (99%), *N*-methyl succinimide (*N*-MSI, 99%), 2-(2-naphthyl)ethylamine hydrochloride ($\text{NpC}_2\text{H}_4\text{NH}_2$ HCL, 97%), 1-pyrenemethylamine hydrochloride (PyCH_2NH_2 HCL, 95%), dimethyl sulfoxide- d_6 (DMSO- d_6 , 99.9 %), dichloromethane (DCM, 99.8%), 1,1,2,2-tetrachloroethane- d_2 (TCE- d_2), sodium acetate (anhydrous), and *tert*-butyl peroxide (98%) were purchased from Sigma-Aldrich and were employed without further purification. Acetic acid (99.7 %, reagent) was purchased from Fischer-Scientific. Two ethylene-propylene copolymers were supplied by Afton Chemical Corporation. One was semicrystalline and the other was amorphous. They were referred to as EP(SM) and EP(AM), respectively.

Fourier Transform Infrared (FTIR). All FTIR spectra were obtained with a Bruker Tensor 27 FTIR spectrophotometer. Polymer solutions prepared with toluene were deposited drop wisely onto a sodium chloride (NaCl) FTIR pellet. The solvent was evaporated under a stream of nitrogen leaving behind a thin polymer film. All samples had an absorbance of less than unity to optimize the signal-to-noise ratio.

Gel Permeation Chromatography (GPC). Weight- and number-average molecular weights and polydispersity indices (PDI) were determined with a Polymer Char high-temperature gel

permeation chromatograph (GPC) instrument at 145 °C using a flow rate of 1 mL/min of 1,2,4-trichlorobenzene (TCB).²⁷ The GPC instrument was equipped with the three following detectors placed in series, namely a differential refractive index, 15° angle light scattering, and differential viscosity detectors. The GPC instrument was also calibrated with polystyrene standards having a narrow molecular weight distribution.

UV-Visible Spectrophotometer (UV-Vis). Absorbances were measured on a Cary 100 UV-Vis spectrophotometer with quartz cells having a 0.1-10 mm path length. Absorbances were measured in the 200–600 nm wavelength range.

Steady-State Fluorescence. A Photon Technology International (PTI) LS-100 steady-state fluorometer equipped with an Ushio UXL-75Xe xenon arc lamp and a PTI 814 photomultiplier detection system was used to acquire the fluorescence spectra. To avoid the inner filter effect when acquiring the fluorescence spectra, a triangular cell was used for front-face geometry measurements at polymer concentrations of 10 g.L⁻¹. For concentrations of 0.01 and 0.1 g.L⁻¹, a square cell was used to acquire the fluorescence spectra with the right-angle geometry. All solutions were deoxygenated for 30-40 minutes under a gentle flow of N₂. Depending on whether the fluorescence experiments were targeting a naphthalene or pyrene chromophore, the solutions were excited at a wavelength of 290 or 344 nm, and the emission spectra were acquired from 300 to 550 nm or 350 to 600 nm, respectively. The fluorescence measurements were also carried out at temperatures ranging from -30 (± 0.2) °C to +25 (± 0.2) °C using a cryostat from Oxford Instruments (Optistat DN) placed in the steady-state fluorometer. Before each measurement, the solutions were heated to room temperature to erase all pre-association history before bringing the solution to the desired temperature. After the set temperature of the cryostat

had been reached, the solution was left in the cryostat for 10 min before any fluorescence spectrum was acquired.

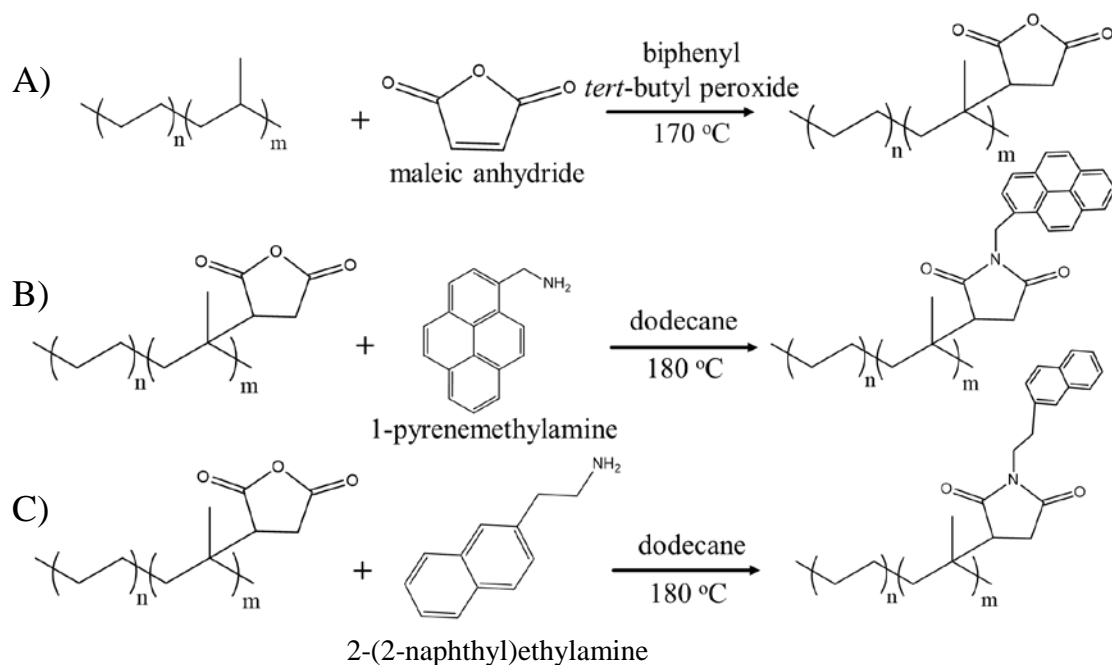
Differential Scanning Calorimeter (DSC). DSC measurements were performed on a TA Q2000 calorimeter calibrated with indium ($T_m = 156$ °C). Samples containing approximately 6 mg of material were weighed and sealed in crimped Tzero aluminum pans prior to analysis. An empty aluminum pan was used as the reference and the chamber was purged with nitrogen at a purge rate of 50 mL/min during analysis. Each sample underwent three temperature cycles: heating from -30 to $+200$ °C, cooling from $+200$ to -30 °C and heating from -30 to $+200$ °C. The temperature scanning rate for all cycles was 10 °C/min and the samples were allowed to equilibrate isothermally for 5 min between each cycle.

Carbon Nuclear Magnetic Resonance (^{13}C NMR). A Bruker 500 MHz high resolution NMR spectrometer was used to acquire the ^{13}C NMR spectra of the EP copolymers in TCE- d_2 at 120 °C.²⁷ A mass of 0.14 g of each sample was dissolved in TCE- d_2 and the solution was placed in an NMR tube. The solution was homogenized by heating the NMR tube in a heating block at 120 °C for a minimum of 4 hrs. The ^{13}C NMR spectra of EP(SM) and EP(AM) are shown in Figure S1. ^{13}C NMR was used to calculate the molar ethylene content of the EP copolymers using a well-documented procedure.²⁸

Proton Nuclear Magnetic Resonance (^1H NMR). A Bruker 300 MHz high resolution NMR spectrometer was used to acquire the ^1H NMR spectra of the model compounds in DMSO- d_6 . A sample concentration of about 10 mg/mL was used to obtain ^1H NMR spectra of the polymer samples with a reasonable signal-to-noise (S/N) ratio.

Labeling of the EP Copolymers. The polymers were first maleated to yield EP-MA²⁹ and then fluorescently labeled with PyCH_2NH_2 and $\text{NpC}_2\text{H}_4\text{NH}_2$ to yield Py-EP and Np-EP,

respectively,²²⁻²⁵ according to the protocols shown in Scheme 1. The synthesis of Py-EP is described in more details hereafter. The EP copolymer (2 g) and biphenyl (60 g) were added into a two-neck round-bottom flask equipped with a condenser. The flask was heated to 160 °C for 12 hrs to ensure good dissolution of the polymers. After complete dissolution, *tert*-butyl peroxide (202 mg, 1.4 mmol) radical initiator was added along with maleic anhydride (MA) (61 mg, 0.8 mmol). The flask was heated to 180-190 °C and left to react under nitrogen for only 4 hrs since longer reaction times led to crosslinking. After the reaction was completed, the hot biphenyl solution was poured into acetone to precipitate the polymer. The polymer was re-dissolved in toluene and precipitated in acetone four times to ensure that no unreacted MA remained in the sample. The drying step was omitted for maleated samples as earlier attempts showed that the maleated samples crosslinked in the vacuum oven.



Scheme 1. Reaction scheme for A) the maleation of the EP copolymer and the labeling of the maleated EP copolymers with B) pyrene and C) naphthalene.

Since the succinic anhydride of EP-MA is moisture sensitive and can react with water to yield less reactive succinic acid, dehydration of the succinic acid was carried out. To this end, purified EP-MA (1 g) and dodecane (60 mL) were placed in a two-neck round-bottom flask equipped with a dean-stark apparatus to remove the water generated during the dehydration conducted at 150-160 °C for 10 hrs under nitrogen atmosphere. Successful dehydration was confirmed by FTIR spectroscopy (Figure 1B). After 10 hrs, PyCH₂NH₂ (185 mg, 0.8 mmol) prepared from PyCH₂NH₂ HCl according to a published procedure³⁰ was added to the reaction vessel and the temperature was kept at 180 °C for another 12 hrs. After the reaction was complete, the reaction mixture was poured into acetone to precipitate out the pyrene-labeled polymer. The precipitate was redissolved in toluene to be precipitated in acetone five more times to remove any unreacted PyCH₂NH₂. The final product was dissolved in toluene and kept in solution to avoid crosslinking of the sample in the dry state. Full conversion of the succinic anhydride (SAH) groups into succinimides after labeling with PyCH₂NH₂ was also confirmed by FTIR spectroscopy (Figure 1C). A similar procedure was also used to label EP-MA with NpC₂H₄NH₂ (Scheme 1C and Figure 1D).

Synthesis of 1-Pyrenemethyl Succinimide (Py-MSI) and 2-(2-Naphthyl)ethyl Succinimide (Np-ESI). 1-Pyrenemethylamine hydrochloride (PyCH₂NH₂·HCl) (0.302 g, 1.11 mmol) was dissolved in water (280 mL) and transferred to a separatory funnel. After addition of three NaOH pellets to the solution, PyCH₂NH₂ was extracted using hexanes (~100 mL) and deionized water.³⁰ Finally, the extracted PyCH₂NH₂ was dried in a vacuum oven at 60 °C for 2-3 hrs.

SAH (214 mg, 2.14 mmol) was dissolved in a solution of acetic acid (13 mL) and sodium acetate (629 mg, 7.68 mmol). Afterward, PyCH₂NH₂ (146 mg, 0.61mmol) was added to the mixture and placed in a round-bottom flask equipped with a water condenser. The solution was heated to 170-180 °C for 12 hrs. The product was then dissolved in toluene (30 mL) and washed with Na₂CO₃ aqueous solution (1 M) 5-6 times followed by 3 water washes. Finally the organic layer was slowly evaporated under a gentle flow of nitrogen. The product was dried in a vacuum oven at 80-90 °C overnight. Py-MSI was further purified by column chromatography using a 70:30 mixture by volume of DCM:hexanes. A similar method was also used to synthesize the Np-ESI. The ¹H NMR spectra of Np-ESI and Py-MSI are shown in Figure S1.

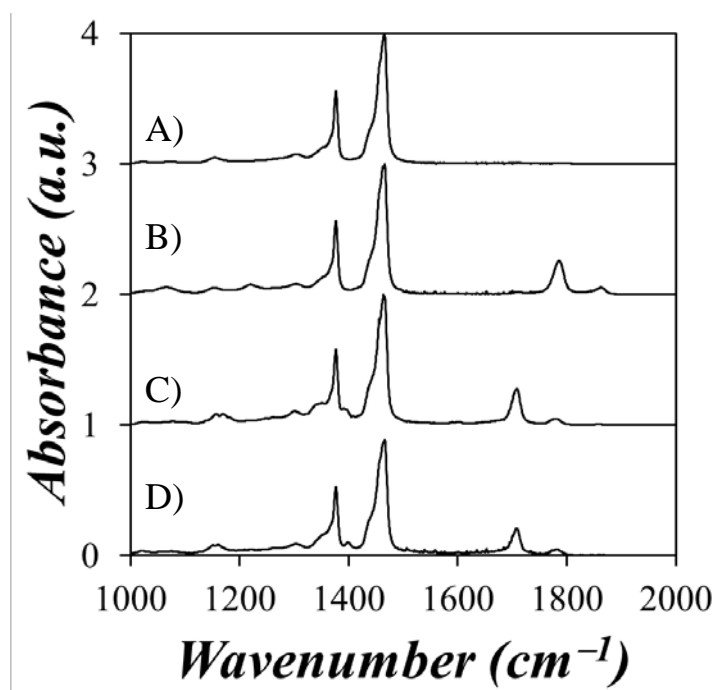


Figure 1. FTIR spectra of A) EP(SM), B) EP(SM)-MA, C) Py(116)-EP(SM), and D) Np(116)-EP(SM).

RESULTS AND DISCUSSION

Considering the importance of characterizing the interpolymer interactions that take place between VIIs in a low polarity solvent, this study aimed to determine the extent to which fluorescence techniques can be applied to characterize the intermolecular associations taking place between fluorescently labeled EP copolymers in toluene as a function of temperature. How this was accomplished is described hereafter.

Chemical Characterization of EP copolymers. The FTIR spectra of EP(SM), EP(SM)-MA, Py(116)-EP(SM), and Np(116)-EP(SM) were acquired and they were shown in Figure 1. The absorption bands at 1462 cm^{-1} and 1379 cm^{-1} in the FTIR spectra of the EP copolymers are due to the methylene and methyl groups of the EP backbone, respectively. Since the FTIR spectrum of a partially hydrated EP-MA sample has two absorption bands at 1710 cm^{-1} and 1785 cm^{-1} due to the carbonyl groups of succinic acid and SAH, respectively, FTIR was applied to ensure that dehydration of EP-MA had taken place. After dehydration, the absorption at 1710 cm^{-1} disappeared, demonstrating that most succinic acids were converted back to their SAH form. The Py(116)-EP(SM) and Np(116)-EP(SM) samples showed a new absorption peak at 1710 cm^{-1} due to the carbonyl groups of the succinimide ring while the peak at 1785 cm^{-1} disappeared due to the reaction of succinic anhydride with the amine group of the fluorescent derivatives (Scheme 1). Since amides absorb between 1600 and 1700 cm^{-1} , the absence of absorbance in this range suggests that most succinic anhydrides cyclized into succinimides upon reaction with the amino-derivative of the fluorophores with minimal formation of amides.

Since the absorption peaks described earlier were well separated in the FTIR spectra, they were integrated and their ratios with respect to the integral of the peak at 1462 cm⁻¹ are listed in Table 1. The Abs(1379 cm⁻¹)/Abs(1462 cm⁻¹) ratio provided a measure of the propylene

Table 1. Summary of the FTIR integral ratios and GPC results for the EP copolymers.

Batch	Polymer Type	$\frac{Abs(1379\text{ cm}^{-1})}{Abs(1462\text{ cm}^{-1})}$	$\frac{Abs(1790\text{ cm}^{-1})}{Abs(1462\text{ cm}^{-1})}$	$\frac{Abs(1710\text{ cm}^{-1})}{Abs(1462\text{ cm}^{-1})}$	M _n (g/mol)	M _w (g/mol)	PDI (M _w /M _n)
	EP(AM)	0.25	-	-	59,000	125,000	2.11
	EP(AM)-MA	0.24	0.18	-	-	-	-
	Py(108)-EP(AM)	0.23	-	0.16	25,000	61,000	2.42
	EP(AM)	0.25	-	-	59,000	125,000	2.11
	EP(AM)-MA	0.25	0.20	-	-	-	-
	Np(108)-EP(AM)	0.25	-	0.17	-	-	-
	EP(SM)	0.21	-	-	55,000	145,000	2.63
	EP(SM)-MA	0.20	0.22	-	-	-	-
	Py(116)-EP(SM)	0.17	-	0.25	33,000	92,000	2.77
	EP(SM)	0.21	-	-	55,000	145,000	2.63
	EP(SM)-MA	0.21	0.21	-	-	-	-
	Py(96)-EP(SM)	0.17	-	0.24	-	-	-
	EP(SM)	0.21	-	-	55,000	145,000	2.63
	EP(SM)-MA	0.19	0.17	-	-	-	-
	Np(116)-EP(SM)	0.17	-	0.24	-	-	-
	EP(SM)	0.21	-	-	55,000	145,000	2.63
	EP(SM)-MA	0.25	0.10	-	-	-	-
	Py(65)-EP(SM)	0.20	-	0.06	-	-	-

content of the EP copolymers. Comparison of the Abs(1379 cm⁻¹)/Abs(1462 cm⁻¹) ratios in Table 1 obtained for the maleated and fluorescently labeled EP copolymers showed that the ratio did not change after the polymer had undergone the different chemical reactions. This observation led to the conclusion that the chemical composition of the EP copolymers in terms of their ethylene and propylene contents was not affected by maleation and the subsequent naphthalene and pyrene labeling. In Table 1, the number in parenthesis after *Py* or *Np* for the pyrene- and naphthalene labeled polymers refers to their dye content expressed in μmol.g⁻¹.

¹³C NMR spectra of EP(SM) and EP(AM) were also acquired and they are shown in Figure S2. The ethylene content of the EP copolymers were calculated according to a published procedure.²⁸ This analysis yielded ethylene contents of 80 and 60 mol% for EP(SM) and EP(AM), respectively. The ethylene content of EP(SM) was found to be larger than that of EP(AM), as expected from the Abs(1379 cm⁻¹)/Abs(1462 cm⁻¹) ratio obtained from the FTIR spectra that equalled 0.20 ± 0.02 and 0.25 ± 0.01 for EP(SM) and EP(AM), respectively, and since a larger ethylene content results in a stronger semicrystalline character for an EP copolymer.

Earlier reports have shown how the SAH content of maleated EP copolymers (EP-MA) can be determined by FTIR after establishing a calibration curve using mixtures of known quantities of the naked EP copolymer and methyl succinic anhydride.³² Unfortunately this method did not apply to EP(SM) and EP(AM) since aromatic solvents like toluene appeared to be the only solvents capable of solubilizing these EP copolymers at room temperature and methyl succinic anhydride was not soluble in toluene, therefore preventing the preparation of homogenous mixtures in toluene of EP copolymers and methyl succinic anhydride.

Consequently, 1-pyrenylmethyl succinimide (Py-MSI) and 2-(2-naphthyl)ethyl succinimide (Np-ESI) were synthesized as model compounds to estimate the SAH content of the EP-MA samples. This estimate of the SAH content assumed that the labeling reaction of the maleated EP copolymer went to completion, a reasonable assumption based on the FTIR spectra shown in Figure 1. The molar extinction coefficient of the model compounds was then measured in toluene and THF based on their absorption spectra (Figures 2 and S3). A summary of the extinction coefficients of Py-MSI and Np-ESI at different wavelengths is given in Table 2.

The molar absorbance coefficients ϵ_{py} and ϵ_{Np} were found to equal 44,800 (± 340) $M^{-1}.cm^{-1}$ at 344 nm and 366 (± 5) $M^{-1}.cm^{-1}$ at 305 nm for Py-MSI and Np-ESI in toluene, respectively. Since ϵ_{Np} at 305 nm was about two orders of magnitude lower than ϵ_{py} at 344 nm, a 100 fold higher polymer concentration was required to measure the naphthalene content of the Np-EP samples.

Table 2. Molar absorbance coefficients for Py-MSI and Np-ESI in toluene and THF.

Model Compound		ϵ at 277 nm ($M^{-1}.cm^{-1}$)	ϵ at 290 nm ($M^{-1}.cm^{-1}$)	ϵ at 305 nm ($M^{-1}.cm^{-1}$)	ϵ at 344 nm ($M^{-1}.cm^{-1}$)
	Toluene	*	*	5,100 \pm 50	44,800 \pm 300
	THF	45,500 \pm 500	4,000 \pm 500	6,100 \pm 300	40,600 \pm 500
	Toluene	*	*	366 \pm 5	0
	THF	4,800 \pm 10	2,600 \pm 10	339 \pm 5	0

* The absorption wall of toluene located between 280-290 nm prevents the determination of the molar absorbance coefficients at wavelengths lower than 290 nm.

High polymer concentrations however caused light scattering, and scattered light interfered with the absorbance peak at 305 nm. Furthermore, the naked EP copolymers themselves showed residual absorbance in the wavelength range where naphthalene absorbed which interfered further with the weak naphthalene absorbance at 305 nm (Figures 2A and S4A). This did not cause a problem for the pyrene-labeled EP copolymers since the much larger ϵ_{py} value at 344 nm enabled the use of much smaller polymer concentrations (Figure 2B and S4B). Consequently, the determination of the naphthalene content of the polymers was not attempted and it was assumed to be similar to that of the corresponding Py-EP samples since they were prepared in a similar manner and showed similar FTIR absorption spectra. As a result, the naphthalene content of Np(116)-EP(SM) and Np(108)-EP(AM) was assumed to be the same as the one determined for Py(116)-EP(SM) and Py(108)-EP(AM), respectively. Comparison of the absorbance at 344 nm for the Py-EP samples and the model compound Py-MSI enabled the determination of the pyrene content λ_{py} of the samples expressed in μmol of pyrene per gram of polymer. The λ_{py} values are provided as the number in parentheses in the sample description. For instance, Py(116)-EP(SM) and Py(108)-EP(AM) have λ_{py} values of 116 and 108 $\mu\text{mol}\cdot\text{g}^{-1}$, respectively. The λ_{py} values are similar thus indicating that on a mass basis, both samples contained a similar number of pyrene labels.

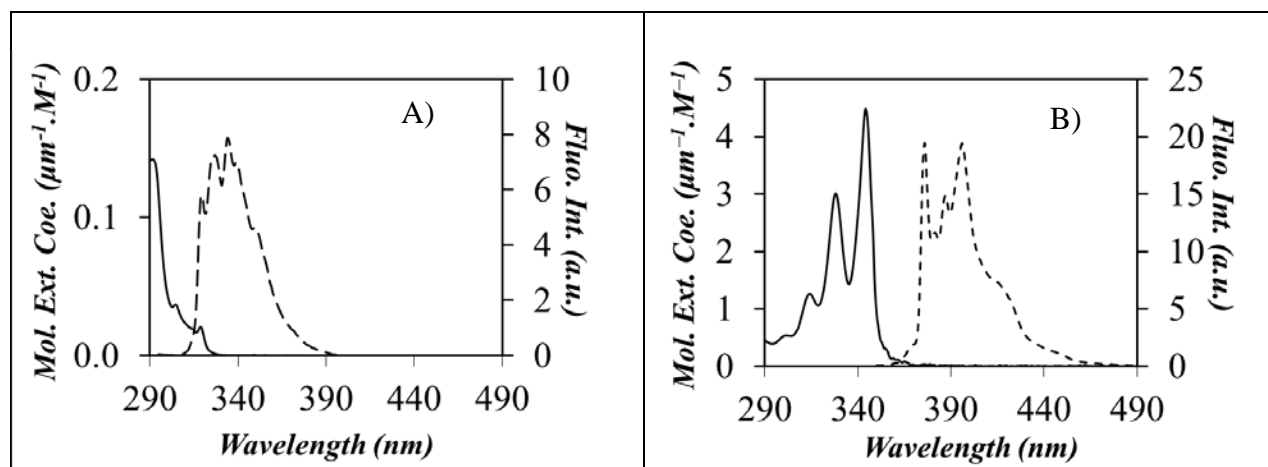


Figure 2. UV-Vis absorption (—) and fluorescence spectra (- - -) of A) 2-(2-naphthyl)ethyl succinimide (Np-ESI) and B) 1-pyrenemethyl succinimide (Py-MSI) in toluene. Note that the absorbance at wavelengths lower than 290 nm is unreliable due to the absorption wall of toluene and were not shown. $[Np-ESI] = 1.78 \times 10^{-3} \text{ mol.L}^{-1}$; $[Py-MSI] = 13 \times 10^{-6} \text{ mol.L}^{-1}$.

One of the advantages of using pyrenyl groups to label macromolecules is that the distribution of these fluorophores along the polymer can be determined qualitatively by measuring the peak-to-valley ratio, or P_A value, from the absorption spectrum of the Py-EP samples¹² or quantitatively by Fluorescence Blob Model analysis of the monomer and excimer decays.²³⁻²⁶ These analyses are described in great detail in SI. The main conclusion of these analyses is that excimer formation occurred principally by diffusive encounters between excited and ground-state pyrene monomers.

Microstructure of the EP Copolymers. Viscosity measurements were carried out between $-10 \text{ }^\circ\text{C}$ and $+20 \text{ }^\circ\text{C}$ for solutions of EP(SM) and EP(AM) in toluene to determine how the intrinsic viscosity $[\eta]$ of the polymers varied as a function of temperature. $[\eta]$ remained constant with temperature for EP(AM) as expected due to the inability of EP(AM) to form microcrystals

in solution and thus undergo drastic conformational changes in solution. For EP(SM), $[\eta]$ decreased sharply with decreasing temperature for temperatures lower than 0 °C (Figure 3A). This decrease in $[\eta]$ for EP(SM) is most likely due to a structural change in the hydrodynamic volume of the polymer coil (V_h) resulting from the formation of crystalline microdomains between long ethylene stretches inside the polymer coil at temperatures lower than 0 °C.²⁻⁴

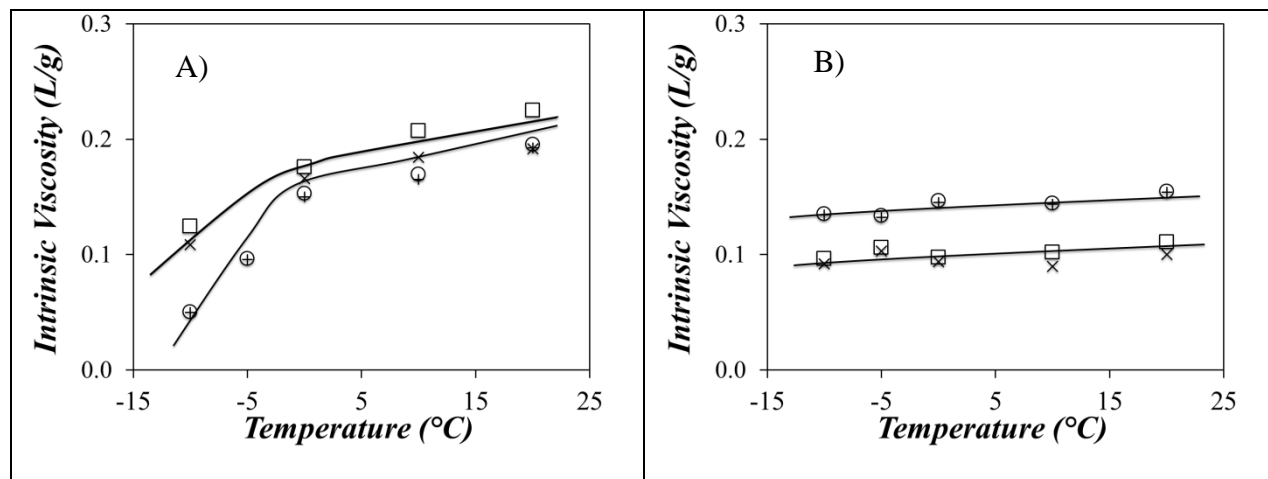


Figure 3. Intrinsic viscosity of A) (□) Py(116)-EP(SM) and (○) EP(SM) obtained by using relative viscosity measurements, and of (×) Py(116)-EP(SM) and (+) EP(SM) obtained by using specific viscosity measurements, and of B) (□) Py(108)-EP(AM) and (○) EP(AM) obtained by using relative viscosity measurements, and of (×) Py(108)-EP(AM) and (+) EP(AM) obtained by using specific viscosity measurements in toluene at various temperatures.

Gel permeation chromatography (GPC) experiments were also conducted on the Py(116)-EP(SM) and Py(108)-EP(AM) samples where the reactive succinic anhydride groups had been capped with 1-pyrenemethylamine. The parameters describing the molecular weight distribution (MWD) of the samples obtained by GPC analysis are listed in Table 1. They show that the number- and weight-average molecular weights decreased and the polydispersity index

(PDI) increased after maleation and pyrene labeling. Consequently, $[\eta]$ was expected to vary from sample to sample due to these alterations in MWD. These changes were more pronounced in the case of Py(108)-EP(AM) suggesting that since the amorphous EP copolymer had more propylene groups, chain cleavage was more likely to happen during maleation.^{32,33} But another explanation could be a change in polymer polarity after pyrene-labeling which might affect the hydrodynamic volume of the coils as the Py-EP copolymers permeate through the GPC column. Despite the variation in MWDs induced by the maleation of the EP copolymers, the trends shown in Figure 3 demonstrate that pyrene labeling did not change the overall $[\eta]$ behavior of the EP copolymers, $[\eta]$ showing a breakpoint at a similar temperature for EP(SM) and little change with temperature for EP(AM).

Finally, differential scanning calorimetry (DSC) experiments were carried out for EP(SM) and EP(AM) samples in the solid state. As shown in Figure S5, a thermal transition due to melting was observed at 31 °C for the semicrystalline sample while no thermal transition was observed for the amorphous sample.

Fluorescence Resonance Energy Transfer (FRET). FRET experiments are typically used to help differentiate whether interactions between macromolecules such as the EP copolymers investigated in this study occur inter- or intramolecularly. To this end, the EP-MA samples were labeled with NpC₂H₄NH₂ and PyCH₂NH₂ which can act as energy donor and acceptor, respectively. The emission spectra of the solutions prepared with Py-EP only, Np-EP only, and mixtures of the Py-EP and Np-EP samples at low (0.1 g.L⁻¹) and high (10 g.L⁻¹) concentration of EP copolymer were acquired to investigate the nature of the interactions taking place between the different polymers. The experiments were conducted in toluene and at temperatures between

-25 and +25 °C, a temperature range that covers the temperatures at which a break point is observed for $[\eta]$ in Figure 3A. Although naphthalene exhibits an absorption peak maximum around 277 nm, an excitation wavelength of 290 nm was chosen in order to minimize the emission of both toluene and the EP copolymers. The fluorescence intensity of the naphthalene monomer, I_{Np} , was calculated by taking the integral of the naphthalene emission intensity between 332 and 338 nm while that of the pyrene monomer, I_{Py} , was obtained from the integral of the pyrene emission intensity between 372 and 378 nm (Figure 4). The I_{Py}/I_{Np} ratio provides a qualitative description of the extent of FRET efficiency, a higher I_{Py}/I_{Np} ratio indicating more efficient FRET and thus stronger intermolecular association. The fluorescence spectra of 9:1 mixtures of Np(116)-EP(SM) and Py(116)-EP(SM) on the one hand and Np(108)-EP(AM) and Py(108)-EP(AM) on the other hand were acquired at different temperatures and at overall polymer concentrations equal to 0.1 and 10 g.L⁻¹. They are shown in Figures 4A and 4B for the 0.1 g.L⁻¹ mixtures of the semicrystalline and amorphous EP copolymers, respectively.

At an overall polymer concentration of 0.1 g.L⁻¹ containing 0.09 g.L⁻¹ of Np-EP and 0.01 g.L⁻¹ of Py-EP, the absorption of these polymer solutions is sufficiently low to avoid direct energy transfer which simplifies the interpretation of the results. EP(SM) in Figure 4A shows large variations in naphthalene and pyrene emission whereby the naphthalene and pyrene emission respectively increases and decreases with increasing temperature. This behaviour is a hallmark of a strong reduction in FRET taking place between Np(116)-EP(SM) and Py(116)-EP(SM) with increasing temperature and demonstrates substantial aggregation of the EP(SM) molecules at low temperature. Much weaker variations were observed for the fluorescence

spectra shown in Figure 4B for the EP(AM) sample reflecting little change in FRET efficiency over the entire temperature range.

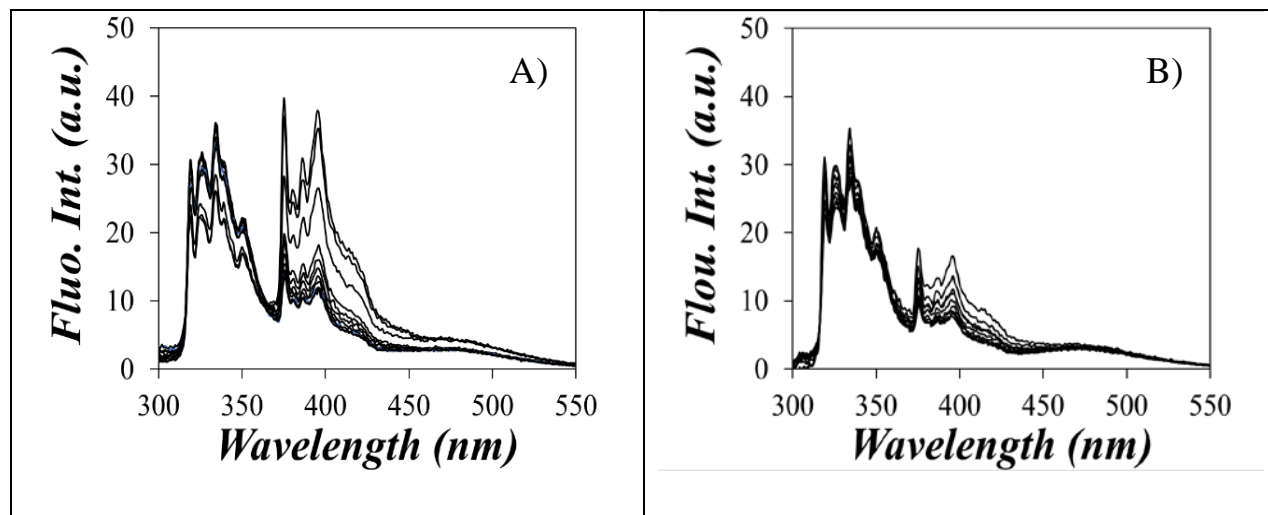


Figure 4. Fluorescence spectra of EP copolymers obtained from of a 9:1 mass ratio mixture of A) Np(116)-EP(SM):Py(116)-EP(SM) and B) Np(108)-EP(AM):Py(108)-EP(AM) as a function of temperature for an overall polymer concentration of 0.1 g.L^{-1} . From top to bottom for the pyrene emission, temperature increases from $-25 \text{ }^{\circ}\text{C}$ to $+25 \text{ }^{\circ}\text{C}$. (solvent: toluene; $\lambda_{\text{ex}} = 290 \text{ nm}$)

When the fluorescence spectra shown in Figure 4 were compared in Figure S6 to the sum of the individual fluorescence spectra of Np-EP and Py-EP adjusted for their respective polymer concentration, a perfect overlap was observed between the fluorescence spectra of the Np-EP and Py-EP mixtures and the sum of the individual spectra at the higher temperature for both the EP(SM) and EP(AM) samples. This observation demonstrated the absence of interpolymeric interactions for both EP copolymers at $25 \text{ }^{\circ}\text{C}$. At low temperature, the mixtures showed a stronger pyrene emission in Figure S6 indicating that both samples underwent FRET, but the pyrene emission was much more pronounced for the EP(SM) than the EP(AM) sample indicating

that interpolymeric interactions at $-20\text{ }^{\circ}\text{C}$ took place more readily in the former than the latter sample.

The picture that emerged from the FRET experiments was that at an overall polymer concentration of 0.1 g.L^{-1} , EP(AM) generates little interpolymeric interactions between -20 and $+25\text{ }^{\circ}\text{C}$, and that EP(SM) forms polymeric aggregates at $-20\text{ }^{\circ}\text{C}$. These results were confirmed by plotting the $I_{\text{Py}}/I_{\text{Np}}$ ratio for Np-EP and Py-EP samples obtained for the 0.1 g.L^{-1} and 10 g.L^{-1} polymer mixtures as a function of temperature in Figure 5. For the 0.1 g.L^{-1} of naphthalene- and pyrene-labeled EP(AM) mixture, $I_{\text{Py}}/I_{\text{Np}}$ showed a continuous decrease with increasing temperature. A somewhat higher $I_{\text{Py}}/I_{\text{Np}}$ ratio was obtained for the 10 g.L^{-1} EP(AM) mixture that behaved similarly as the ratio obtained for the 0.1 g.L^{-1} EP(AM) concentration whereby the $I_{\text{Py}}/I_{\text{Np}}$ ratio decreased also continuously with increasing temperature. The plots of $I_{\text{Py}}/I_{\text{Np}}$ versus temperature obtained with both the 0.1 and 10 g.L^{-1} EP(SM) mixtures differed markedly from those obtained with the EP(AM) mixtures by showing a pronounced break point in the mid-temperature range of Figure 5. Since an increase in $I_{\text{Py}}/I_{\text{Np}}$ reflects an increase in intermolecular interactions, the sharp increase in $I_{\text{Py}}/I_{\text{Np}}$ with decreasing temperature observed at -10 and $-5\text{ }^{\circ}\text{C}$ for, respectively, the 0.1 and 10 g.L^{-1} EP(SM) solutions indicates a dramatic enhancement in interpolymeric association, a consequence of the formation of crystalline microdomains as expected from the intrinsic viscosity measurements. It is worth pointing out that the polymer concentrations used for the intrinsic viscosity measurements ranged between 0.5 and 3.5 g.L^{-1} and are thus intermediate between the two EP(SM) concentrations used for the FRET experiments. It is thus quite satisfying that the onset temperature between -10 and $-5\text{ }^{\circ}\text{C}$ for intermolecular associations observed by FRET matches relatively well that found for the drop in

intrinsic viscosity observed in Figure 3 for EP(SM). The 0.1 g.L⁻¹ solution used in the FRET experiment being more dilute required a lower temperature of -10 °C to worsen the solvent quality toward EP(SM) sufficiently to induce EP(SM) to associate intermolecularly.

Pyrene Excimer Formation. While FRET experiments demonstrate the existence of interpolymeric association, a quantitative measure of the actual level of intermolecular association between fluorescently labeled macromolecules is usually quite challenging to obtain by FRET. By comparison, the molar fraction of pyrene labels forming pyrene excimer intermolecularly (f_{inter}) can be determined in a straightforward manner as illustrated hereafter.

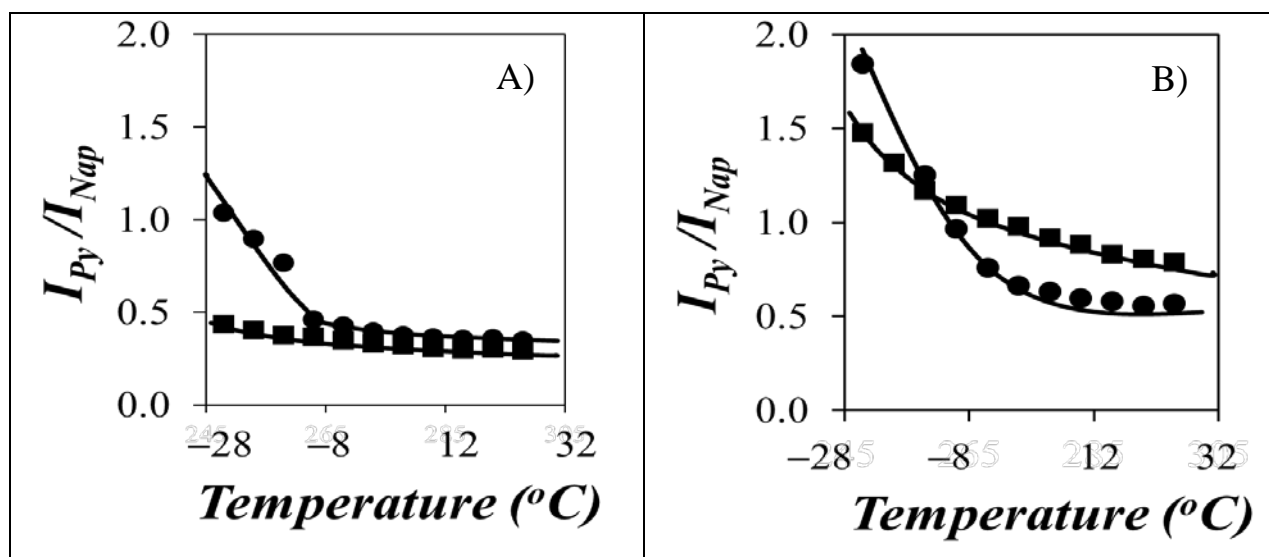


Figure 5. I_{Py}/I_{Nap} ratio for mixtures of a 9:1 mass ratio of (■) Np(108)-EP(AM):Py(108)-EP(AM) and (●) Np(116)-EP(SM):Py(116)-EP(SM) as a function of temperature. A) 0.1 g.L⁻¹ and B) 10 g.L⁻¹.

In the fluorescence spectrum of pyrene-labeled macromolecules (PLMs), the excited pyrene monomer emission is characterized by several sharp peaks between 360 nm and 425 nm,

whereas the pyrene excimer features a broad and structureless emission centered at 480 nm.²¹ The fluorescence intensity of the pyrene excimer (I_E) and monomer (I_M) can be calculated by integrating the fluorescence spectrum over the wavelength ranges between 372 and 379 nm and between 500 and 530 nm, respectively. The fluorescence intensity ratio I_E/I_M is widely accepted to be directly proportional to the local pyrene concentration $[Py]_{loc}$ as described by Equation 1.³⁴

$$I_E/I_M = K(T) \times [Py]_{loc} \quad (1)$$

In Equation 1, the multiplication factor $K(T)$ is a function of the quantum yields of the pyrene monomer and excimer, the bimolecular rate constant of excimer formation, and the acquisition geometry and the instrument response of the fluorometer. As such, $K(T)$ is expected to vary with temperature according to the activation energy of the different photophysical parameters associated with the process of pyrene excimer formation. According to this relationship, an increase in I_E/I_M observed at a same temperature reflects an increase in $[Py]_{loc}$ which would result from intermolecular interactions. In turn, intermolecular interactions can be the result of an increase in the concentration of the PLM or a change in the solvent quality toward the macromolecule. If experimental conditions can be determined where a PLM of interest undergoes both intra- and intermolecular interactions, its fluorescence spectrum will yield the ratio $I_E/I_M \left(\begin{smallmatrix} \text{inter\&} \\ \text{intra} \end{smallmatrix} \right)$ whereas if the PLM undergoes solely intramolecular interactions, the fluorescence spectrum will yield the ratio $I_E/I_M(\text{intra})$. In turn, the ratios $I_E/I_M \left(\begin{smallmatrix} \text{inter\&} \\ \text{intra} \end{smallmatrix} \right)$ and $I_E/I_M(\text{intra})$ are equal to $K(T) \times [Py]_{loc} \left(\begin{smallmatrix} \text{inter\&} \\ \text{intra} \end{smallmatrix} \right)$ and $K(T) \times [Py]_{loc}(\text{intra})$, respectively, so that the

molar fraction of pyrene labels forming excimer intermolecularly (f_{inter}) can be determined from Equation 2.

$$f_{\text{inter}} = \frac{[Py]_{loc} \left(\begin{smallmatrix} \text{inter \&} \\ \text{intra} \end{smallmatrix} \right) - [Py]_{loc} (\text{intra})}{[Py]_{loc} \left(\begin{smallmatrix} \text{inter \&} \\ \text{intra} \end{smallmatrix} \right)} = \frac{I_E / I_M \left(\begin{smallmatrix} \text{inter \&} \\ \text{intra} \end{smallmatrix} \right) - I_E / I_M (\text{intra})}{I_E / I_M \left(\begin{smallmatrix} \text{inter \&} \\ \text{intra} \end{smallmatrix} \right)} \quad (2)$$

In Equation 2, f_{inter} is also equal to the molar fraction of macromolecules that interact intermolecularly. We note with interest that the constant $K(T)$ introduced in Equation 1 cancels out in the expression of f_{inter} , a welcomed simplification as the determination of the activation energies of all the photophysical parameters related to the process of excimer formation with randomly labeled polymers would be a challenging task.

Experimentally, the ratio $I_E/I_M \left(\begin{smallmatrix} \text{inter \&} \\ \text{intra} \end{smallmatrix} \right)$ can be obtained in a straightforward manner, simply by acquiring the fluorescence spectrum of a PLM under conditions where it undergoes intermolecular interactions. In the case of the EP(SM) sample where intrinsic viscosity measurements established that the hydrodynamic volume decreased substantially with decreasing temperature thus reflecting a decrease in the solvent quality toward EP(SM), an increase in polymer concentration and a decrease in temperature both contribute to induce intermolecular interactions. For such a sample, $I_E/I_M(\text{intra})$ is more challenging to determine as EP(SM) has an inherent tendency to associate intermolecularly even at low polymer concentration as the FRET experiments have established for EP(SM) concentrations as low as 0.1 g.L⁻¹. To ensure that intramolecular excimer formation would only be observed for the determination of $I_E/I_M(\text{intra})$, the fluorescence spectrum of dilute (0.01 g.L⁻¹) solutions of the PLMs was acquired in the presence of 10 g.L⁻¹ of the unlabeled macromolecule. Under such conditions, the large excess of

unlabeled macromolecule ensures that the formation of intermolecular polymeric aggregates would only incorporate one PLM per aggregate thus ensuring that the fluorescence spectrum of such a solution would report solely on pyrene excimer formed intramolecularly from PLMs isolated in large aggregates of unlabeled macromolecules.

Since engine oils are polymer solutions containing a few wt% of VII, the fluorescence spectra of 10 g.L⁻¹ Py(116)-EP(SM) and Py(108)-EP(AM) solutions in toluene were acquired as a function of temperature and they are shown in Figure 6. In the case of Py(108)-EP(AM), the fluorescence intensity of the excimer (I_E) at 480 nm remained more or less constant with temperature, but the fluorescence intensity of the pyrene monomer (I_M) at 375 nm increased continuously with decreasing temperature, a consequence of the increase in solvent viscosity associated with a decrease in temperature which reduces pyrene excimer formation by diffusion and increases the monomer quantum yield. The behavior of Py(116)-EP(SM) was similar to that of Py(108)-EP(AM) at temperatures lower and higher than -10 °C whereby I_E decreased a little and I_M increased more substantially and continuously with decreasing temperature. Compared to these gradual variations in fluorescence signal with decreasing temperature, I_E showed a step-increase at -10 °C for Py(116)-EP(SM), a consequence of an increase in intermolecular associations taking place for that sample around -10 °C.

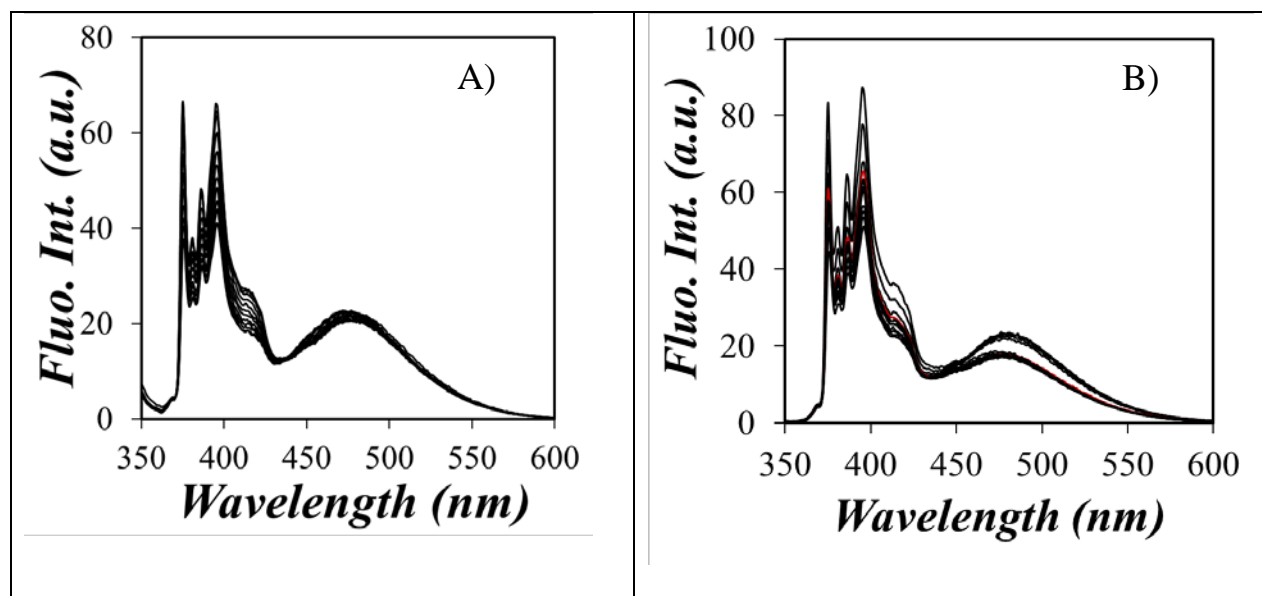


Figure 6. Fluorescence spectra of A) Py(108)-EP(AM) (10 g.L^{-1}) and B) Py(116)-EP(SM) (10 g.L^{-1}). From top to bottom: temperature increases from $-35 \text{ }^{\circ}\text{C}$ to $+25 \text{ }^{\circ}\text{C}$. Solvent is toluene and $\lambda_{\text{ex}} = 344 \text{ nm}$.

Beside the fluorescence experiments conducted in Figure 6, the fluorescence spectra of toluene solutions containing 0.01 g.L^{-1} Py-EP were also acquired as a function of temperature for the EP(SM) and EP(AM) samples as well as the fluorescence spectra of a solution in toluene containing 10 g.L^{-1} of unlabeled EP copolymer and 0.01 g.L^{-1} Py-EP to obtain the ratio $I_E/I_M(\text{intra})$. The I_E/I_M ratios of all the fluorescence spectra were calculated and they were plotted in Figure 7 as a function of temperature. For all Py(108)-EP(AM) solutions, the I_E/I_M ratio increased continuously with increasing temperature in Figures 7B and 7D. This is the expected behavior for pyrene-labeled macromolecules at temperatures lower than $35 \text{ }^{\circ}\text{C}$.^{2,35} In this temperature regime, the dissociation rate constant of the pyrene excimer is negligible and I_E/I_M is proportional to the product of the bimolecular rate constant for excimer formation by diffusion

(k_{diff}) and $[Py]_{\text{loc}}$. Since EP(AM) is soluble in toluene at all temperatures with a constant polymer coil volume based on the intrinsic viscosity experiments (Figure 3), $[Py]_{\text{loc}}$ does not change much with temperature and the increase in I_E/I_M with increasing temperature reflects the increase in k_{diff} associated with the decrease in the solvent viscosity associated with an increase in temperature.

Interestingly EP(SM) yields a very different plot of I_E/I_M as a function of temperature in Figures 7A and 7C. For both the 10 g.L^{-1} Py(116)-EP(SM) and 0.01 g.L^{-1} Py(96)-EP(SM) solutions without an excess of unlabeled EP(SM), an increase in solution temperature induces first an increase in I_E/I_M , followed by a decrease in I_E/I_M at intermediate temperatures, before the expected increase in I_E/I_M resumes at higher temperatures. The anomalous behavior observed for Py(116)-EP(SM) and Py(96)-EP(SM) at intermediate temperatures reflects a change in excimer formation which could have two origins. The first origin would be the result of the volume expansion of the polymer coil happening as the compact crystalline microdomains of EP(SM) melt, thus decreasing $[Py]_{\text{loc}}$. The second cause would be the dissociation of Py-EP(SM) aggregates happening at intermediate temperatures which would also result in a decrease in $[Py]_{\text{loc}}$.

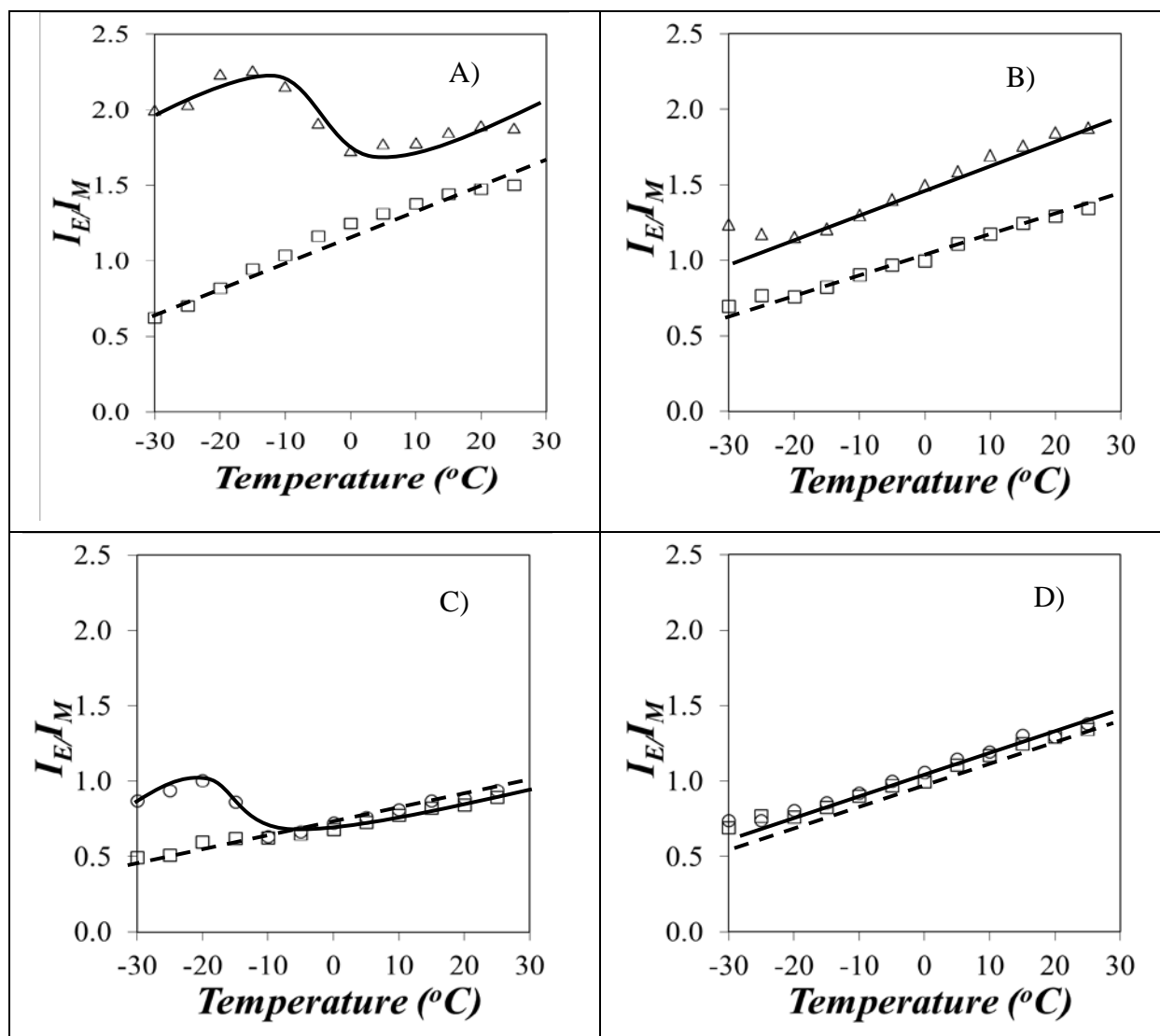


Figure 7. I_E/I_M versus temperature. A) (Δ) Py(116)-EP(SM) (10 g.L^{-1}), (\square) mixture of Py(116)-EP(SM) (0.01 g.L^{-1}) and EP(SM) (10 g.L^{-1}). B) (Δ) Py(108)-EP(AM) (10 g.L^{-1}), (\square) mixture of Py(108)-EP(AM) (0.01 g.L^{-1}) and EP(AM) (10 g.L^{-1}). C) (\circ) Py(96)-EP(SM) (0.01 g.L^{-1}), (\square) mixture of Py(96)-EP(SM) (0.01 g.L^{-1}) and EP(SM) (10 g.L^{-1}). D) (\circ) Py(108)-EP(AM) (0.01 g.L^{-1}), (\square) mixture of Py(108)-EP(AM) (0.01 g.L^{-1}) and EP(AM) (10 g.L^{-1}).

The FRET experiments discussed earlier have confirmed that intermolecular associations take place for EP(SM) at low temperature, but a reduction in the overall dimension of the polymer coil happening in the low temperature regime cannot be ruled out. In any case, both effects contribute to the decrease in $[Py]_{loc}$ that is probed through the decrease in the I_E/I_M ratio with increasing temperature observed at intermediate temperatures. We also note with interest that the break point seen in the I_E/I_M profile shown in Figures 7A and 7C matches that observed earlier with another pyrene-labeled semicrystalline EP copolymer implying that this behavior seems to be representative of such polymers.²

In the presence of 10 g.L⁻¹ excess EP copolymer, all 0.01 g.L⁻¹ Py-EP solutions showed a continuous increase in I_E/I_M with increasing temperature. This behaviour is expected for a pyrene-labeled macromolecule where excimer formation occurs intramolecularly and with a rate constant that increases with increasing temperature. This behaviour confirms that the presence of 10 g.L⁻¹ excess unlabeled EP copolymer prevents intermolecular interactions so that these trends yield $I_E/I_M(\text{intra})$ in Equation 2. Equation 2 was applied to the trends shown in Figure 7 to yield f_{inter} that was plotted as a function of temperature in Figure 8. Compared to the complex trends obtained with the I_E/I_M -versus-temperature profiles in Figure 7, the f_{inter} -versus-temperature plots shown in Figure 8 are much simpler to interpret. For all EP(AM) solutions, f_{inter} remained constant with temperature as expected from a polymer for which temperature does not induce intermolecular associations or conformational changes. At a low 0.01 g.L⁻¹ Py(108)-EP(AM) concentration, little-to-no intermolecular interactions should be observed for this non-associative polymer as is indeed the case in Figure 8B that yields an f_{inter} value of 0.03 ± 0.03 over the entire temperature range. Increasing the Py(108)-EP(AM) concentration to 10 g.L⁻¹ in Figure 8B increases the probability of pyrene-pyrene encounters in the solution and diffusive

intermolecular excimer formation results in the higher f_{inter} value of 0.31 ± 0.02 . The transition induced by the formation of crystalline microdomains for the Py(116)-EP(SM) solutions appears now quite clearly in Figure 8A where the two regimes at temperature below and above the transition can be easily assigned. For the 10 g.L^{-1} Py(116)-EP(SM) solution, f_{inter} increases from 0.23 ± 0.03 at high temperature to 0.62 ± 0.07 at low temperature, the inflexion point of the transition being at $T = -5 \pm 3 \text{ }^\circ\text{C}$. For the more dilute Py(96)-EP(SM) solution of 0.01 g.L^{-1} , no intermolecular interactions are taking place at high temperatures where f_{inter} equals 0.04 ± 0.02 . After passing through an inflexion point at $T = -15 \pm 3 \text{ }^\circ\text{C}$, f_{inter} increases to 0.43 ± 0.03 at low temperature. The shift in the transition temperature from -5 to $-15 \text{ }^\circ\text{C}$ when the concentration is reduced from 10 to 0.01 g.L^{-1} reflects the difficulty for two polymer coils to encounter each other at such a low concentration. At a Py(96)-EP(SM) concentration of 0.01 g.L^{-1} , the quality of the solvent needs to be made considerably worse for interpolymeric associations to take place. This explains why these interactions are observed at a lower temperature for this polymer concentration. The f_{inter} values obtained in the different temperature regimes have been listed in Table 3.

To investigate the robustness of the procedure, a Py(65)-EP(SM) sample was also synthesized with a lower pyrene content λ_{Py} of $65 \text{ } \mu\text{mol.g}^{-1}$. f_{inter} was determined as a function of temperature as shown in Figure 8A. Interestingly, despite the difference in pyrene content for the two Py-EP(SM) samples, the procedure used to obtain f_{inter} appears to yield a same trend regardless of pyrene content. This result demonstrates the validity of the procedure which appears to report on the solution behaviour of the EP copolymers and is not influenced by differences in pyrene labeling.

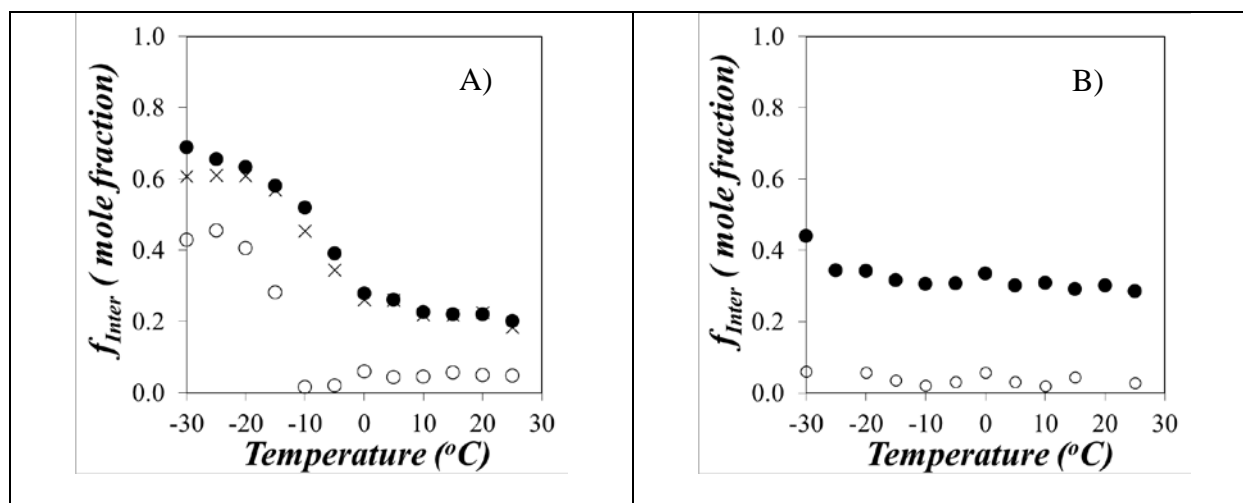


Figure 8. Molar fraction f_{inter} of pyrene labeled EP copolymers forming excimer intermolecularly for A) (●) Py(116)-EP(SM) and (×) Py(65)-EP(SM) at a concentration of 10 g.L⁻¹, and (○) Py(96)-EP(SM) at a concentration of 0.01 g.L⁻¹ and B) Py(108)-EP(AM) at a concentration of (●) 10 g.L⁻¹ and (○) 0.01 g.L⁻¹.

Table 3. Summary of the molar fraction (f_{inter}) obtained for the different Py-EP samples.

	λ_{py}	Concentration (g.L ⁻¹)	Temperature Range -30 to -10 $^{\circ}C$	Temperature Range -5 to 25 $^{\circ}C$
	116	10	0.62 ± 0.07	0.23 ± 0.03
	65	10	0.57 ± 0.07	0.24 ± 0.03
Py-EP(AM)	108	10	0.31 ± 0.02	
Py-EP(SM)	96	0.01	0.43 ± 0.03	0.04 ± 0.02
Py-EP(AM)	108	0.01	0.03 ± 0.03	

CONCLUSIONS

Two different EP copolymers were maleated and subsequently labeled with 1-pyrenemethylamine or 2-(2-naphthyl)ethylamine. FTIR and DSC measurements performed in the solid state confirmed that EP(SM) was semicrystalline while EP(AM) was amorphous. The FTIR measurements also confirmed that the chemical composition of the copolymers in terms of ethylene and propylene content was not affected by the maleation and labeling reaction, although GPC experiments showed that some chain scission took place after these reactions. Nevertheless, intrinsic viscosity experiments indicated that the solution behaviour of the fluorescently labeled EP copolymers was similar to that of the unmodified polymers.

To probe the interactions taking place between polymer chains at the molecular level, fluorescence experiments based on FRET and excimer formation were conducted on the pyrene- and naphthalene-labeled EP copolymers. The FRET experiments showed that low temperatures induced interpolymeric interactions in toluene for both EP copolymers, but that these interactions were much stronger for the EP(SM) sample. While informative, the FRET experiments did not yield a parameter that would qualify the strength of these interpolymeric interactions.

Fluorescence experiments based on pyrene excimer formation were implemented to achieve this goal. The pyrene-labeled EP(AM) and EP(SM) samples yielded very different profiles of I_E/I_M versus temperature. While I_E/I_M increased continuously with increasing temperature for Py(108)-EP(AM) as would be expected for any pyrene-labeled macromolecule in solution, a much more complex profile was found for Py(116)-EP(SM) with a marked transition in the same temperature range where a breakpoint had been observed for the profile of the intrinsic viscosity versus temperature in Figure 3. Comparison of the I_E/I_M profiles obtained with 10 g.L⁻¹ toluene solution of pyrene-labeled EP copolymer with a toluene solution

containing 0.01 g.L^{-1} of pyrene-labeled EP and 10 g.L^{-1} of unlabeled polymer yielded f_{inter} , the molar fraction of pyrene labels that formed excimer intermolecularly. Although the derivation of f_{inter} was based on the determination of the I_E/I_M ratio that depended on the activation energy of numerous photophysical processes, this complicated temperature-dependency was fortuitously eliminated in the calculation of f_{inter} . Plots of f_{inter} as a function of temperature showed that f_{inter} did not depend much on temperature for a 10 g.L^{-1} EP(AM) solution in toluene remaining constant at 0.31 ± 0.02 . For the 10 g.L^{-1} EP(SM) solution, two clear regimes were identified depending on whether the solution temperature was below or above $-5 \text{ }^\circ\text{C}$ where f_{inter} took a large or small value of about 0.60 ± 0.07 or 0.23 ± 0.03 , respectively. The increase in f_{inter} at low temperature observed for EP(SM) was attributed to the intermolecular formation of microcrystals. Finally the trend obtained with Py(116)-EP(SM) was duplicated with Py(65)-EP(SM), an EP(SM) copolymer prepared with a lower pyrene content to demonstrate that the results obtained with f_{inter} were describing the behaviour of the polymer itself and were insensitive to the pyrene content of the polymer.

In summary, this study has demonstrated that FRET and pyrene excimer formation that occur over distances of several nanometers respond to changes in the local polymer concentration induced by a worsening of the solvent quality toward the polymer. But whereas FRET provides qualitative evidence that intermolecular interactions are taking place, analysis of the fluorescence spectra acquired with the pyrene-labeled EP copolymers yielded f_{inter} , a parameter that describes quantitatively the strength of interpolymeric associations. Considering how strongly the rheological properties of polymer solutions are affected by interpolymeric associations, the ability to describe the strength of these interpolymeric associations via a single

parameter should prove extremely valuable to the numerous scientists aiming to rationalize the complex rheological behaviour of solutions of associating polymers.

ACKNOWLEDGMENTS

The authors thank Afton Chemical Corporation for their generous financial support of this research, Dr. Joao Soares for conducting the GPC experiments, Dr. Ralph Dickhout for running the DSC experiments, and Ms. Janet Venne for performing the ^{13}C NMR experiments.

SUPPORTING INFORMATION

^1H NMR spectra of Np-ESI and Py-MSI; ^{13}C NMR spectra of EP(AM) and EP(SM); absorption spectra of the dyes; DSC traces for the polymers; overlap of the fluorescence spectra of the mixtures of Np-EP and Py-EP with the sum of the individual spectra of Np-EP and Py-EP adjusted for their respective polymer concentrations; detailed analysis of the absorption spectra and fluorescence decays of the Py-EP samples.

REFERENCES

- (1) Pawlak, Z. In *Tribochemistry of lubricating oils*; Elsevier: Poland, 2003; Vol. 45.
- (2) Zhang, M.; Duhamel, J. Study of the Microcrystallization of Ethylene-Propylene Random Copolymers in Solution by Fluorescence. *Macromolecules* **2007**, *40*, 661-669.
- (3) Rubin, I. D.; Sen, A. Solution Viscosities of Ethylene-Propylene Copolymers in Oils. *J. Appl. Polym. Sci.* **1990**, *40*, 523-530.

- (4) Sen, A.; Rubin, I. D. Molecular Structures and Solution Viscosities of Ethylene-Propylene Copolymers. *Macromolecules* **1990**, *23*, 2519-2524.
- (5) LaRiviere, D.; Asfour, A. A.; Hage, A.; Gao, J. Viscometric Properties of Viscosity Index Improvers in Lubricant Base Oil over a Wide Temperature Range. Part I: Group II Base Oil. *Lubr. Sci.* **2000**, *12*, 133-143.
- (6) Tanveer, S.; Prasad, R. Enhancement of Viscosity Index of Mineral Base Oils. *Indian J. Chem. Technol.* **2006**, *13*, 398-403.
- (7) Mihaljuš S. V.; Podobnik, M.; Bambić, J. Engine Oil Viscosity Index Improver Behaviour at Extended Shear Stability. *Fuels Lubr.* **2008**, *47*, 118-128.
- (8) Kucks, M. J.; Ou-Yang, H. D.; Rubin, I. D. Ethylene-Propylene Copolymer Aggregation in Selective Hydrocarbon Solvents. *Macromolecules* **1993**, *26*, 3846-3850.
- (9) Port, W. S.; O'Brien, J. W.; Hansen, J. E.; Swern, D. Viscosity Index Improvers for Lubricating Oils. Polyvinyl Esters of Long-Chain Fatty Acids. *Ind. & Eng. Chem.* **1951**, *43*, 2105-2107.
- (10) Rudnik, L. R. In *Chemistry and Application*; Barbadsz, E. A.; Lamb, G. D. Eds.; Lubricant Additives; CRC Press, Boca Raton: Florida, 2003; pp 458-490.
- (11) Mortier, R. M.; Malcolm, F. F.; Orszulik, S. T. In *Chemistry and Technology of Lubricants*; Springer: London, 2009.
- (12) Winnik, F. M.; Regismond, S. T. A. Fluorescence Methods in the Study of the Interactions of Surfactants with Polymers. *Colloid Surf. A. Physicochem. Eng. Aspects* **1996**, *118*, 1-39.
- (13) Naciri, J.; Weiss, R. G. New Methods for the Determination of Dopant Site Distributions and Dopant Rates of Diffusion in Polymer Films: Emission from Pyrenyl Groups Covalently Attached to Low-Density Polyethylene. *Macromolecules* **1989**, *22*, 3928-3936.

- (14) He, Z.; Hammond, G. S.; Weiss, R. G. New Methods for the Determination of Dopant Site Distributions and Dopant Rates of Diffusion in Polymer Films with Covalently Attached Anthryl Groups: Fluorescence Quenching by *N,N*-dimethylaniline in Unstretched, Stretched, and Swelled Films. *Macromolecules* **1992**, *25*, 1568-1575.
- (15) Wang, C.; Weiss, R. G. Method for Hydroxylation and Esterification of Interior Sites of Polyolefinic Films. *Macromolecules* **1999**, *32*, 7032-7039.
- (16) Cigogna, F.; Coiai, S.; Pinzino, C. ; Ciardelli, F.; Passaglia, E. Fluorescent Polyolefins by Free Radical Post-Reactor Modification with Functional Nitroxides. *React. Funct. Polym.* **2012**, *72*, 695-702.
- (17) Jao, T.-C.; Mishra, M. K.; Rubin, I. D. Studies on Ethylene-Propylene Copolymer in Hydrocarbon Solvents by Fluorescence Probe Method. *Macromol. Reports* **1992**, *29*, 283-292.
- (18) Mortier, R. M.; Malcolm, F. F.; Orszulik, S. T. In *Chemistry and Technology of Lubricants*; Springer: London, 2009.
- (19) Anghel, D. F.; Alderson, V.; Winnik, F. M.; Mizusaki, M.; Morishima, Y. Fluorescent Dyes as Model 'Hydrophobic Modifiers' of Polyelectrolytes: A Study of Poly(Acrylic Acid)s Labeled with Pyrenyl and Naphthyl Groups. *Polymer* **1998**, *39*, 3035-3044.
- (20) Yamamoto, H.; Mizusaki, M.; Yoda, K.; Morishima, Y. Fluorescence Studies of Hydrophobic Association of Random Copolymers of Sodium 2-(Acrylamido)-2-Methylpropanesulfonate and N-Dodecylmethacrylamide in Water. *Macromolecules* **1998**, *31*, 3588-3594.
- (21) Birks, J. B.; Dyson, D. J.; Munro, I. H. Excimer Fluorescence. II. Lifetime Studies of Pyrene Solutions. *Proc. Royal Soc. Series A, Math. Phys. Sci.* **1963**, *275*, 575-588.

- (22) Németh, S.; Jao, T.-C.; Fendler, J. Concentration- and Solvent-Dependent Excimer Formation of 1-Pyrenemethanamine, Covalently Attached to Maleic Anhydride-Grafted Ethylene-Propylene Copolymers. *Macromolecules* **1994**, *27*, 5449-5456.
- (23) Vangani, V.; Drage, J.; Mehta, J.; Mathew, A. K.; Duhamel, J. Maleated Ethylene-Propylene Random Copolymers: Determination of the Microstructure and Association Level by Fluorescence Spectroscopy. *J. Phys. Chem. B* **2001**, *105*, 4827-4839.
- (24) Zhang, M.; Duhamel, J. Effect of Solvent Quality Toward the Association of Succinimide Pendants of a Modified Ethylene-Propylene Copolymer in Mixtures of Toluene and Hexane. *Macromolecules* **2005**, *38*, 4438-4446.
- (25) Zhang, M.; Duhamel, J. Study of Maleated Ethylene-Propylene Copolymers by Fluorescence: Evidence for Succinimide Induced Polar Associations in an Apolar Solvent. *Eur. Polym. J.* **2008**, *44*, 3005-3014.
- (26) Duhamel, J. New Insights in the Study of Pyrene Excimer Fluorescence to Characterize Macromolecules and their Supramolecular Assemblies in Solution. *Langmuir* **2012**, *28*, 6527-6538.
- (27) Alshaiban, A.; Soares, J. B. P. Effect of Hydrogen and External Donor on Propylene Polymerization Kinetics with a 4th Generation Ziegler-Natta Catalyst. *Macro. React. Eng.* **2012**, *6*, 265-274.
- (28) Randall, J. C. A Review of High Resolution Liquid ¹³Carbon Nuclear Magnetic Resonance Characterizations of Ethylene-Based Polymers. *J. Macro. Sci. Rev. Macromol. Chem. Phys.* **1989**, *C29*, 201-317.

- (29) Heinen, W.; Rosenmüller, C. H.; Wenzel, C. B.; De Groot, H. J. M.; Lugtenburg, J. ¹³C NMR Study of the Grafting of Maleic Anhydride onto Polyethene, Polypropene, and Ethene–Propene Copolymers. *Macromolecules* **1996**, *29*, 1151-1157.
- (30) Nemeth, S.; Jao, T.-C.; Fendler, J. H. Excimer Formation in 1-Pyrenyl-methane-amine *Photochem. Photobiol. A: Chem.* **1994**, *78*, 22-235.
- (31) Walch, E.; Gaymans, R. J. Telechelic Polyisobutylene with Unsaturated End Groups and with Anhydride End Groups. *Polymer* **1994**, *35*, 1774-1778.
- (32) Gaylord, N. G.; Mishra, M. K. Nondegradative Reaction of Maleic Anhydride and Molten Polypropylene in the Presence of Peroxides. *J. Polym. Sci.: Polym. Let. Ed.* **1983**, *21*, 23-30.
- (33) Gaylord, N. G.; Mehta, M.; Mehta, R. Degradation and Cross-linking of Ethylene-propylene Copolymer Rubber on Reaction with Maleic Anhydride and/or Peroxides. *J. Appl. Polym. Sci.* **1987**, *33*, 2549-2558.
- (34) Cuniberti, C.; Perico, A. Intramolecular Excimer Formation in Polymers. *Eur. Polym. J.* **1980**, *16*, 887-893.
- (35) Stevens, B.; Ban, M. I. Spectrophotometric Determination of Enthalpies and Entropies of Photoassociation for Dissolved Aromatic Hydrocarbons. *Trans. Far. Soc.* **1964**, *60*, 1515–1523.